Interaction-induced Dimension Reduction for Bound States in Microwave-Shielded Ultracold Molecules

Haitian Wang,^{1,2,*} Tingting Shi,^{1,*} and Xiaoling Cui^{1,†}

¹Beijing National Laboratory for Condensed Matter Physics, Institute of Physics, Chinese Academy of Sciences, Beijing, 100190, China ²School of Physical Sciences, University of Chinese Academy of Sciences, Beijing 100049, China (Dated: November 14, 2025)

We investigate tetratomic and hexatomic bound states of ultracold molecules dressed by an elliptic microwave field. We show that these bound states can be accurately described by effective one-dimensional (1D) models incorporating high-order angular fluctuations, despite the physical system is in three-dimensional (3D) free space. By comparing with exact solutions of the full 3D system, we identify the validity region of such 1D description in the parameter plane of ellipticity and coupling strength of microwave field. The hard-core character of these effective models enables a duality between bosonic and fermionic molecules in real and spectral space, while their momentum distributions remain distinct. Our results have demonstrated an effective dimension reduction in microwave-shielded molecular systems, which is purely due to the intrinsic interaction anisotropy rather than any external confinement. Extending to large systems, our results suggest a self-bound single-molecule array as the ground state of both bosonic and fermionic molecular gases.

I. INTRODUCTION

Few-body physics plays an indispensable role in ultracold gases, where the formation of few-body bound states governs both the practical stability of the system and the emergence of novel many-body phases. For instance, the existence of Efimov trimers[1, 2], which exhibit discrete scaling invariance and binding energies sensitive to a short-range three-body parameter, typically induces significant three-body loss in atomic gases[3–5]. In contrast, a distinct class of universal bound states exists, whose properties are independent of short-range details and are determined by only a few physical parameters [6– 14]. These clusters are expected to be stable against inelastic collisions and are responsible for universal manybody phases with intriguing higher-order correlations [15– 19. While all these bound states have been extensively investigated in atomic systems with short-range interactions, their counterparts in long-range interacting systems remain largely unexplored.

As an ideal platform for simulating long-range interactions, ultracold dipolar molecules have recently gained rapid developments thanks to the technique of microwave shielding [20–31]. This method creates a large repulsive shielding core (on the order of $100-1000~a_B$, where a_B is the Bohr radius), which prevents molecules from approaching closely and thus strongly suppresses inelastic two-body losses. These developments have enabled milestone achievements such as Fermi degeneracy [23] and Bose-Einstein condensation [28–30] of molecular gases. Furthermore, by tuning the ellipticity and coupling strength of the microwave field, experiments have successfully observed scattering resonances [24], tetratomic

bound states[25, 31] in fermionic molecules, and self-bound droplets in bosonic systems[29, 30]. Theoretically, research has predominantly focused on two-body scattering[32–38], fermionic superfluids[34] and bosonic droplets[39–42]. However, the exploration of fundamental few-body physics in dipolar systems has only been at its infancy[43–48]. Drawing on the established importance of few-body physics in atomic systems, a comprehensive understanding of its role in dipolar molecules is highly demanded, for both precisely controlling collisional stability and guiding the search for novel many-body phases therein.

A number of previous studies have explored fewbody physics in long-range interacting dipolar sys-For example, the Efimov effect and universal bound states have been studied in bosonic[43, 46] and fermionic[44, 46] systems, taking an interaction combining isotropic short-range and anisotropic long-range potentials. However, such interaction potential differs significantly, in both its long- and short-range behavior, from the microwave-shielded potential relevant to ultracold molecules. Adopting a similar shielding potential. Ref. [45] has studied the bound state formation in 2D molecules. Recently, as the first attempt of few-body problem in 3D microwave-shielded molecules, we considered the case of extreme interaction anisotropy under a highly elliptic microwave field [48]. There, effective onedimensional (1D) models incorporating the lowest-order angular fluctuations were established to describe universal bound states, revealing a strong suppression of Efimov physics and the emergence of a Bose-Fermi duality. Nevertheless, in realistic experiments of ultracold molecules, microwave fields are generally with small ellipticities, as this is essential for a strong shielding effect in suppressing two-body losses [49]. For this practical regime, it remains an open question whether the effective models and bound state properties identified in Ref. [48] are still applicable.

In this work, we investigate the bound states of ultra-

^{*} These authors contributed equally to this work.

[†] xlcui@iphy.ac.cn

cold molecules under realistic microwave shielding conditions, specifically focusing on small ellipticities. For this regime, we develop an improved effective 1D model that incorporates high-order angular fluctuations. This model yields accurate predictions for both the tetratomic binding energy and the Born-Oppenheimer potential in three-molecule sector. By comparing our model with exact numerical solutions, we identify its validity regime in the parameter plane of ellipticity and coupling strength of microwave field. Remarkably, we find the 1D description remains valid even at small ellipticities for typical microwave coupling strengths on the order of tens of MHz. Within this valid regime, the Bose-Fermi duality in real and spectral space is preserved. The quantum statistics of the molecules, however, remain distinguishable through their momentum distributions. Furthermore, we find that hexatomic molecules are generally more deeply bound than tetratomic ones across a wide range of ellipticities and microwave couplings. For the ground state, the hexatomic bound state is well-approximated by two linked tetratomic states. This structure, when extended to larger systems, suggests the formation of a self-bound "single-molecule array" for both bosonic and fermionic molecules.

Our work demonstrates an improved effective 1D model to accurately describe the bound state formation in 3D ultracold molecules. Crucially, this dimensional reduction stems purely from the intrinsic anisotropy of interaction potential, a mechanism qualitatively distinct from conventional method of external confinement. The resulting universal few-body physics are fundamentally different from those in short-range interacting atomic systems and should be directly observable in current experiments with ultracold molecules.

II. INTERACTION MODEL

We consider ultracold molecules dressed by an elliptic microwave field $\mathbf{E} = Ee^{i(kz-\omega t)}(\mathbf{e}_{+}\cos\xi + \mathbf{e}_{-}\sin\xi) + c.c.$, where $\mathbf{e}_{\pm} = \mp(\mathbf{e}_{x} \pm i\mathbf{e}_{y})$ and ξ is the elliptic angle. The inter-molecule potential can be written as[34]

$$V(\mathbf{r}) = \frac{C_3}{r^3} \left(3\cos^2\theta - 1 + 3f_{\xi}\sin^2\theta\cos(2\phi) \right) + \frac{C_6}{r^6} \left(1 - \left[\cos^2\theta + f_{\xi}\sin^2\theta\cos(2\phi)\right]^2 \right).$$
(1)

Here $\mathbf{r}=(r,\theta,\phi)$ is the relative distance; $f_{\xi}=\sin(2\xi)$; $C_3=\frac{d^2}{48\pi\epsilon_0(1+\delta_r^2)},~C_6=\frac{d^4}{128\pi^2\epsilon_0^2\Omega(1+\delta_r^2)^{3/2}}~(\delta_r=\frac{|\delta|}{\Omega})$ with Ω and δ , respectively, denoting the frequency and detuning of microwave field; d is dipole momentum that defines dipole length $l_d\equiv\frac{m}{\hbar^2}\frac{d^2}{48\pi\epsilon_0}$. Specifically, $l_d=1.1,~2.6,~8.3(10^4a_0)$ for NaK[23–25], NaCs[27–29] and NaRb[26, 30] molecules, respectively. In comparison, the size of shielding core in these systems is much smaller ($\sim~100-1000a_0$ for Ω of tens of MHz), which determines the mean inter-molecule distance in a bound

state. Therefore, in this work we take the length unit as $l_u=l_d/20$, and accordingly the energy unit as $E_u=\frac{\hbar^2}{ml_u^2}$. Take NaK molecule as an example, we have $\hbar\Omega/E_u\approx 157$ at a typical $\Omega=(2\pi)30 \mathrm{MHz}$. In addition, we fix $\delta_r=0.2$ throughout this work.

Note that although the shielding core ($\sim 100-1000a_0$) is much smaller than the dipole length (l_d) , it is comparable to the typical length scale of few-molecule bound states and therefore its anisotropy cannot be neglected. This distinguishes our work from previous studies of few-body physics in dipolar systems [43, 44, 46], which assumed an isotropic s-wave potential at short range. Moreover, in contrast to our previous work on highly elliptic case[48], here we focus on small, finite ellipticities of microwave field, specifically with $\xi \leq \pi/12$. Such small ξ not only validate $V(\mathbf{r})$ as a good approximation for the real interaction potential[34], but also produce a strong shielding effect that efficiently stabilizes the system against two-body losses [49]. In this regime, the repulsive $1/r^6$ shielding core exists in all directions, while the long-range $-1/r^3$ attraction remains most pronounced along y, see Fig.1(a). We will establish effective 1D models along this direction to describe the bound state formation in this system.

III. DERIVATIONS OF EFFECTIVE 1D MODELS

To construct an effective model along y, one must integrate out angular fluctuations in the perpendicular directions. For smaller ξ , the effect of angular fluctuations is stronger due to the weaker attraction of $V(\mathbf{r})$ along y. In this case, it is necessary to include high-order angular fluctuations beyond the lowest-order terms considered previously[48]. In the following, we derive these effective models with high-order angular fluctuations for tetratomic and hexatomic molecular systems.

A. Tetratomic system

In the basic two-molecule level with relative coordinate $\mathbf{r} = (r, \theta, \phi)$, we can expand

$$\theta = \theta^{(0)} + \delta\theta, \quad \phi = \phi^{(0)} + \delta\phi, \tag{2}$$

where $\theta^{(0)} = \pi/2$, $\phi^{(0)} = \pm \pi/2$ represent $\pm y$ direction, and $\delta\theta, \delta\phi$ denote angular fluctuations beyond this direction. As shown in Fig.1(b1,b2), such angular fluctuations lead to the increase of $V(\mathbf{r})$ along z and x directions. Here, we expand $V(\mathbf{r})$ and kinetic term $H_k(\mathbf{r}) = -\hbar^2 \nabla_{\mathbf{r}}^2/m$ up to the fourth-order of fluctuation modes:

$$V(\mathbf{r}) = V^{(0)} + V^{(2)} + V^{(4)};$$
 (3)

$$H_k(\mathbf{r}) = H_k^{(0)} + H_k^{(2)} + H_k^{(4)}.$$
 (4)

In above expansion, $\{V^{(0)}, H_k^{(0)}\}$ are bare terms that are independent of $\delta\theta$ and $\delta\phi$, and $\{V^{(2)}, H_k^{(2)}\}$ and $\{V^{(4)}, H_k^{(4)}\}$ are respectively the second- and fourthorder corrections due to angular fluctuations, see explicit expressions in Methods.

tetratomic wavefunction under adiabatic representation[50–52] can be written as

$$\Psi_2(\mathbf{r}) = \frac{1}{r} \sum_{\nu} F_{\nu}(y) \psi_{\nu}(y; \delta\theta, \delta\phi), \tag{5}$$

with $y = r \sin \phi^{(0)}$ the reduced 1D coordinate. By integrating out the angular fluctuations in ψ_{ν} , we can obtain an effective Hamiltonian governing the reduced 1D wavefunction F_{ν} . Here we neglect the coupling between different ν and only keep the ground state level ($\nu = 0$). Moreover, since different orders of fluctuations contribute differently to the effective potential, we adopt a separate treatment as below. First, we solve $\psi_{\nu=0}$ from

$$\left(H_k^{(2)} + V^{(2)}\right)\psi_0(y;\delta\theta,\delta\phi) = U_{\text{eff}}^{(2)}(y)\psi_0(y;\delta\theta,\delta\phi), \quad (6)$$

which gives (denoting $r \equiv |y|$)

$$U_{\text{eff}}^{(2)}(r) = \left(\sqrt{1 + f_{\xi}} + \sqrt{2f_{\xi}}\right) \sqrt{\frac{\hbar^2}{m} \left(\frac{3C_3}{r^5} + \frac{2f_{\xi}C_6}{r^8}\right)}.$$
(7)

Here $U_{\text{eff}}^{(2)}$ is the zero-point energy of harmonic oscillator expanded by quadratic terms of $\delta\theta$ and $\delta\phi$. It is the lowest-order correction to 1D potential, which scales as $U_{\rm eff}^{(2)}\sim 1/r^4$ at $r\to 0$, as previously also derived for $\xi=\pi/4[48]$. In this work, we take one step further to evaluate the high-order correction as

$$U_{\text{eff}}^{(4)}(r) = \langle \psi_0 | H_k^{(4)} + V^{(4)} | \psi_0 \rangle.$$
 (8)

Analytical expression of $U_{\rm eff}^{(4)}$ is presented in Methods. At $r \to 0$, $|U_{\rm eff}^{(4)}| \sim 1/r^2 \ll 1/r^4 \sim U_{\rm eff}^{(2)}$; namely, the high-order correction of effective potential is much smaller than the lowest-order one. This in turn validates the separate treatment of $U_{\mathrm{eff}}^{(n)}$ as above. The final effective 1D Hamiltonian for tetratomic sys-

tem can be written as:

$$\left(-\frac{\hbar^2}{m}\frac{\partial^2}{\partial y^2} + V^{(0)} + U_{\text{eff}}^{(2)} + U_{\text{eff}}^{(4)}\right)F_0(y) = E_2^{1D}F_0(y). \tag{9}$$

Here $V^{(0)}$ is the bare interaction along y, and $U_{\text{eff}}^{(2)}$, $U_{\text{eff}}^{(4)}$ are respectively the second- and fourth-order corrections from angular fluctuations. A typical comparison of interaction potentials up to different orders of corrections is shown in Fig. 1(c).

Hexatomic system

For a hexatomic system of three molecules, the angular fluctuations of three tetratomic pairs can entangle with one another. Consequently, the effective potential of hexatomic system generally cannot be formulated as a direct summation of three independent tetratomic potentials. In this section, we derive the effective 1D potential for two hexatomic systems. The first is heavy-heavylight system, where we focus on the induced heavy-heavy potential mediated by the light particle in the Born-Oppenheimer (BO) limit. This exactly solvable case serves as a benchmark for justifying the validity of effective 1D approach to hexatomic problem. We then proceed with the second system of three identical molecules.

1. Heavy-heavy-light system

In the BO framework, we consider two localized heavy molecules at $\pm \mathbf{R}/2$, which interact with a moving light molecule via the microwave-shielded potential. Hamiltonian of the light object is

$$H_L(\mathbf{r}) = -\frac{\hbar^2}{2m} \nabla_{\mathbf{r}}^2 + V(\mathbf{r} - \frac{\mathbf{R}}{2}) + V(\mathbf{r} + \frac{\mathbf{R}}{2}), \quad (10)$$

giving the Schrödinger equation

$$H_L(\mathbf{r})\Psi_L(\mathbf{r}) = V_{BO}(\mathbf{R})\Psi_L(\mathbf{r}).$$
 (11)

Here the eigen-energy $V_{\rm BO}(\mathbf{R})$ can be viewed as the effective potential between two heavy molecules induced by the movement of the light one. Considering the directional anisotropy of V in (1), we focus on the case when \mathbf{R} is along y direction, such that the bound state formation is most favored in this system.

Similar to the tetratomic case in (2), here we define two angular fluctuation modes, $\delta\theta$ and $\delta\phi$, for the light molecule with coordinate $\mathbf{r} = (r, \theta, \phi)$. Then H_L in (10) can be expanded up to different orders of these modes. Explicitly, the zeroth- and second-order expansion terms can be expressed as

$$\begin{split} H_L^{(0)}(r) &= \frac{1}{2} H_k^{(0)}(r) + \sum_{\sigma = \pm} V^{(0)}(r_\sigma); \\ H_L^{(2)}(y, \delta\theta, \delta\phi) &= \frac{1}{2} H_k^{(2)}(r, \delta\theta, \delta\phi) + \sum_{\sigma = \pm} V^{(2)}(r_\sigma, \delta\theta_\sigma, \delta\phi_\sigma), \end{split}$$
(12)

where $H_k^{(n)}$ and $V^{(n)}$ are respectively the *n*-th order expansions of kinetic and interaction potentials in Eqs. (3,4), and the factor 1/2 in front of $H_k^{(n)}$ is because of the mass difference in this case. Moreover, we have defined $\mathbf{r}_{\pm} \equiv \mathbf{r} \pm \mathbf{R}/2$, and $(r_{\pm}, \theta_{\pm}, \phi_{\pm})$ is its spherical coordinate with angular fluctuations $\{\delta\theta_{\pm}, \delta\phi_{\pm}\}$. Given **R** along y, $\{\delta\theta_+, \delta\phi_+\}$ can be related to $\{\delta\theta, \delta\phi\}$ via

$$\delta\theta_{+} = r\delta\theta/r_{+}, \quad \delta\phi_{+} = y\delta\phi/r_{+};$$
 (13)

with $y = r \sin \phi^{(0)}$ the projection of **r** along y direction. After a straightforward algebra, we find that $H_L^{(2)}$ is composed by two separate harmonic oscillators in terms of $\delta\theta$ and $\delta \phi$, see Methods.

The wavefunction of light molecule, $\Psi_L(\mathbf{r})$, can be written as a similar form of (5), with the reduced 1D wavefunction F_{ν} and angular part ψ_{ν} . Again we only focus on the ground state level ($\nu = 0$) and require $\psi_{\nu=0}$

$$H_L^{(2)}\psi_0(y;\delta\theta,\delta\phi) = U_{\text{L:eff}}^{(2)}(y)\psi_0(y;\delta\theta,\delta\phi). \tag{14}$$

The zero-point energy $U_{\rm L;eff}^{(2)},$ see expression in Methods, is the light-induced heavy-heavy interaction up to the lowest-order angular fluctuations. For $\xi = \pi/4$, it recovers the result in Ref. [48]

The evaluation of high-order angular fluctuations, however, is quite complicated due to very complex form of high-order expansion term $(H_L^{(4)})$ as a function of $\{y, \delta\theta, \delta\phi\}$. Considering $H_L^{(4)}$ only contributes to a smaller correction as compared to $H_L^{(2)}$, we simplify its evaluation by neglecting the angular entanglements between different heavy-light pairs. In this way, the fourthorder contribution can be approximated as

$$U_{\text{L:eff}}^{(4)}(y) = u_{\text{eff}}^{(4)}(r_{+}) + u_{\text{eff}}^{(4)}(r_{-}), \tag{15}$$

where $u_{\text{eff}}^{(4)}$ is the fourth-order correction of a heavy-light pair with relative distance $r_{\pm} = |y \pm R/2|$, see Methods. Finally, the reduced 1D equation for the light molecule

$$\left(-\frac{\hbar^2}{2m}\frac{\partial^2}{\partial y^2} + V^{(0)}(r_+) + V^{(0)}(r_-) + U^{(2)}_{L;eff} + U^{(4)}_{L;eff}\right)I$$

$$= E_L^{1D}F_0(y).$$

Here the eigen-energy $E_L^{\rm 1D}$ is exactly the light-induced potential V_{BO} at a given heavy-heavy separation R.

Three identical molecules

Similarly, we can set up an effective 1D model for hexatomic system of three identical molecules. In the centerof-mass frame, three identical molecules $\{\mathbf{r}_1,\mathbf{r}_2,\mathbf{r}_3\}$ can be described by two relative coordinates $\mathbf{r} = \mathbf{r}_2 - \mathbf{r}_1$ and $\rho = \frac{2}{\sqrt{3}}(\mathbf{r}_3 - (\dot{\mathbf{r}}_1 + \mathbf{r}_2)/2)$. The Hamiltonian can be written as

$$H_3 = -\frac{\hbar^2}{m} (\nabla_{\mathbf{r}}^2 + \nabla_{\boldsymbol{\rho}}^2) + V(\mathbf{r}) + V(\mathbf{r}_+) + V(\mathbf{r}_-) (17)$$

with $\mathbf{r}_{\pm} = \frac{\mathbf{r}}{2} \pm \frac{\sqrt{3}\boldsymbol{\rho}}{2}$. Denoting the angular fluctuations of $\mathbf{r}, \boldsymbol{\rho}$ as $\{\delta\theta_r, \delta\phi_r\}$ and $\{\delta\theta_\rho, \delta\phi_\rho\}$, one can then expand H_3 up to a given order of fluctuations. Specifically, the zeroth- and second-order terms read

$$H_3^{(0)}(r,\rho) = H_k^{(0)}(r) + H_k^{(0)}(\rho) + V^{(0)}(r) + \sum_{\sigma=\pm} V^{(0)}(r_\sigma);$$

$$H_3^{(2)}(y_r, \delta\theta_r, \delta\phi_r; y_\rho, \delta\theta_\rho, \delta\phi_\rho)$$

$$= H_k^{(2)}(r, \delta\theta_r, \delta\phi_r) + H_k^{(2)}(\rho, \delta\theta_\rho, \delta\phi_\rho)$$

$$+ V^{(2)}(r, \delta\theta_r, \delta\phi_r) + \sum_{\sigma = \pm} V^{(2)}(r_\sigma, \delta\theta_\sigma, \delta\phi_\sigma). \tag{18}$$

Here $y_r = r \sin \phi_r^{(0)}$, $y_\rho = \rho \sin \phi_\rho^{(0)}$ are respectively the projection of \mathbf{r} , $\boldsymbol{\rho}$ along y direction; $(r_\sigma, \theta_\sigma, \phi_\sigma)$ is the spherical coordinate of \mathbf{r}_{σ} (here $\sigma = \pm$), with angular fluctuations $\{\delta\theta_{\sigma}, \delta\phi_{\sigma}\}$ following

$$\delta\theta_{\sigma} = \frac{r\delta\theta_{r} + \sigma\sqrt{3}\rho\delta\theta_{\rho}}{2r_{\sigma}};$$

$$\delta\phi_{\sigma} = \frac{y_{r}\delta\phi_{r} + \sigma\sqrt{3}y_{\rho}\delta\phi_{\rho}}{2r_{\sigma}}.$$
(19)

As shown in Methods, $H_3^{(2)}$ is composed by two independent harmonic oscillators in terms of $\{\delta\theta_r, \delta\theta_\rho\}$ and $\{\delta\phi_r, \delta\phi_\rho\}$, while within each oscillator the two modes are entangled with each other. Such an entangled oscillator can be diagonalized following the approach in Ref. [48].

For three molecules with a given projection ordering along y, their wavefunction can be written as

$$\Psi_3(\mathbf{r}, \boldsymbol{\rho}) = \frac{1}{r\rho} \sum_{\nu} F_{\nu}(y_r, y_{\rho}) \psi_{\nu}(y_r, y_{\rho}; \delta\theta_r, \delta\phi_r, \delta\theta_{\rho}, \delta\phi_{\rho}),$$
(20)

Up to the lowest-order fluctuations, the ground state $(\psi_{\nu=0})$ of the angular part satisfies

$$H_3^{(2)}\psi_0 = U_{3,\text{eff}}^{(2)}(y_r, y_\rho)\psi_0.$$
 (21)

Here the eigen-energy $U_{3;\text{eff}}^{(2)}$ is just the effective 1D po- $\left(-\frac{\hbar^2}{2m}\frac{\partial^2}{\partial u^2} + V^{(0)}(r_+) + V^{(0)}(r_-) + U^{(2)}_{\text{L;eff}} + U^{(4)}_{\text{L;eff}}\right) F_0(y) \text{ tential induced by the lowest-order angular fluctuations,}$ as previously studied for $\mathcal{E} = \pi/4$ in Ref.[48]. as previously studied for $\xi = \pi/4$ in Ref. [48].

> (16) Following the strategy in evaluating high-order correction to heavy-heavy-light system, here we neglect the entanglement between different tetratomic pairs and write the fourth-order correction as

$$U_{3:\text{eff}}^{(4)}(y_r, y_\rho) = U_{\text{eff}}^{(4)}(r) + U_{\text{eff}}^{(4)}(r_+) + U_{\text{eff}}^{(4)}(r_-), \quad (22)$$

where $r = |y_r|$, $r_{\pm} = |y_r \pm \sqrt{3}y_{\rho}|/2$ and $U_{\text{eff}}^{(4)}$ follows (8). Finally, the effective 1D equation for three identical molecules is written as

$$\left[-\frac{\hbar^2}{m} \left(\frac{\partial^2}{\partial y_r^2} + \frac{\partial^2}{\partial y_\rho^2} \right) + V^{(0)}(r) + V^{(0)}(r_+) + V^{(0)}(r_-) + U^{(2)}_{3;\text{eff}} + U^{(4)}_{3;\text{eff}} \right] F_0(y_r, y_\rho) = E_3^{1D} F_0(y_r, y_\rho). \tag{23}$$

Here $U_{3;\rm eff}^{(2)}$ and $U_{3;\rm eff}^{(4)}$ are the effective 1D potentials from the lowest- and high-order angular fluctuations, respectively, which scale as $1/r^4$ and $-1/r^2$ whenever pairwise molecules come close with distance $r \to 0$. Their explicit expressions are presented in Methods.

NUMERICAL RESULTS

Tetratomic bound state

We have solved the tetratomic bound states using both exact numerical methods and the effective 1D model,

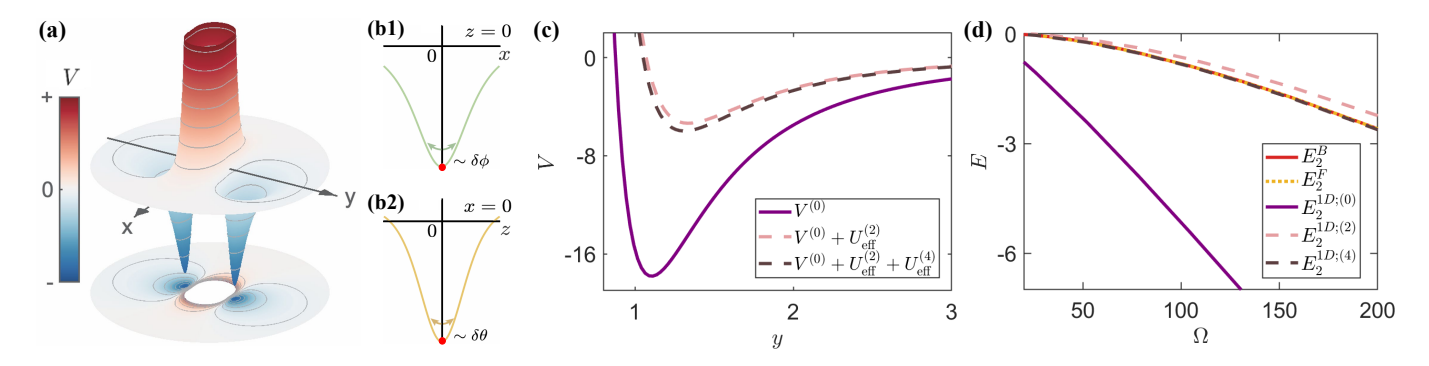


FIG. 1. Interaction potential and tetratomic bound state of microwave-shielded molecules with elliptic angle $\xi = \pi/12$. (a) Typical interaction potential $V(\mathbf{r})$ at xy plane (z=0). (b1,b2) Schematics of angular fluctuations of $V(\mathbf{r})$ along $x (\sim \delta \phi)$ and $z (\sim \delta \theta)$ directions. The red points denote the minimum of V when \mathbf{r} locates at y axis (x=z=0). (c) Comparison of different 1D potentials (along y) at $\hbar\Omega/E_u=157$. $V^{(0)}$ is the bare potential, and $U^{(2)}_{\mathrm{eff}}$, $U^{(4)}_{\mathrm{eff}}$ are the effective potentials from the lowest- and fourth-order angular fluctuations, respectively. (d) Tetratomic binding energies as functions of Ω . E_2^B and E_2^F are from exact solutions of bosonic and fermionic molecules, and $E_2^{1D;(n)}$ is from effective 1D model up to the n-th order angular fluctuations. The units of length, energy and Ω are respectively l_u , E_u and E_u/\hbar .

which allow us to identify the parameter regime for the validity of 1D description. To obtain exact solutions, we have expanded the tetratomic wavefunction in terms of eigenstates in momentum (k) and angular momentum

(l,m) space and diagonalize the Hamiltonian using $\{klm\}$ basis [48]. Meanwhile, we have diagonalized the effective 1D model (9) directly in real space to obtain the bound state solution.

Take a small ellipticity $\xi = \pi/12$ as an example, in Fig.1(d) we show the binding energies of tetratomic ground state from exact solutions and from effective 1D models up to different orders of angular fluctuations. The corresponding 1D potentials along y are shown in Fig.1(c). We can see that the bare potential $(V^{(0)})$ significantly overestimates the binding energy, while the effective potential with lowest-order correction $(V^{(0)} + U_{\text{eff}}^{(2)})$ yields a substantial improvement. Remarkably, by further incorporating the fourth-order correction $(U_{\text{eff}}^{(4)})$, the effective 1D model achieves excellent agreement with exact results across a wide range of Ω . We emphasize that including high-order corrections is more crucial for smaller ξ , where the interaction anisotropy is less pronounced and the fluctuations beyond y direction can affect the bound state formation more significantly.

Despite accurately predicting the tetratomic state in Fig.1(d), the effective 1D model does not always preform well, particularly for shallow bound states with small binding energies[48]. In the following, we identify the validity regime of effective 1D model by comparing with exact solutions of tetratomic system. Before proceeding, we note that the hard-core nature of 1D model (9) enables an important eigen-state property as Bose-Fermi duality, i.e., bosonic and fermionic molecules share identical eigen-spectrum and real-space distribution. This occurs because, for a given spatial ordering of particles on a 1D line, the system wavefunction is independent of statistics, with different statistics only determining the sign change of the wavefunction in other spatial ordering

sectors. Such duality has been previously pointed out in short-range interacting 1D systems[53, 54] and long-range interacting dipolar systems[46, 48]. Here, we utilize Bose-Fermi duality as a criterion for judging the validity of 1D model.

In Fig.2(a), we show a magnified comparison of tetratomic binding energies between exact results and 1D predictions based on (9), for a fixed $\xi = \pi/12$ and varying Ω . We can see that near the threshold of bound state formation, the 1D model fails for both bosonic and fermionic systems, as evidenced by visible deviations between the exact (E_2^B, E_2^F) and 1D (E_2^{1D}) results. Physically, this failure arises because these shallow bound states exhibit a 3D character. For instance, the emergence of E_2^B for bosonic molecules is associated with an s-wave resonance where the scattering length diverges, $a_s \to \infty$. As explored in detail for $\xi=\pi/4$ [48], the shallow bound states near resonance well follow $E_2^B=-\hbar^2/(ma_s^2)$, and thus these states expand isotropically in free space rather than being confined essentially to one direction. For fermionic molecules, the shallow tetratomic bound state resides in the p-wave channel, which emerges at a larger Ω than the bosonic one. However, as Ω increases, both bosonic and fermionic systems gradually depart from the 3D regime and begin to exhibit Bose-Fermi duality, consistent with the 1D description. As shown in Fig.2(a), as Ω increases, E_2^B and E_2^F converge and tend to merge into a single line predicted by E_2^{1D} . To quantify this convergence, we

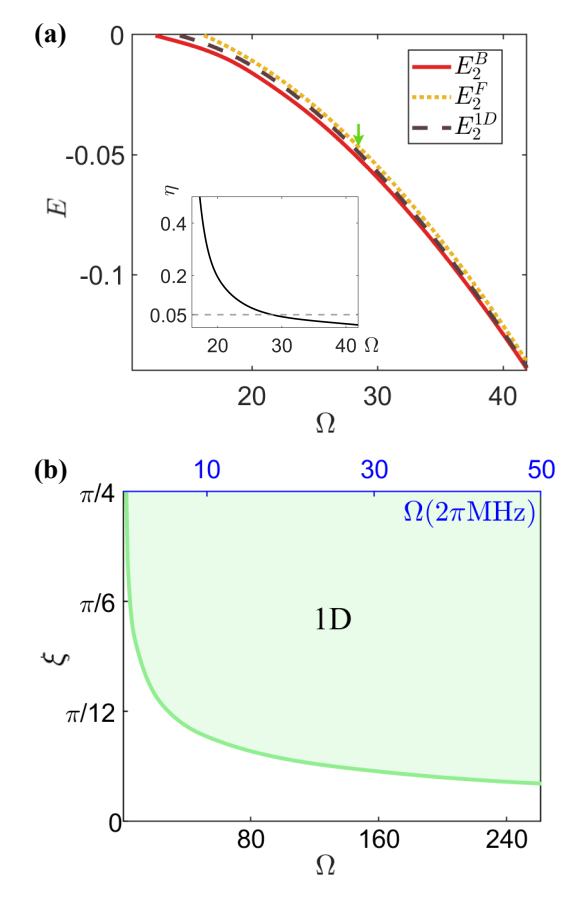


FIG. 2. Validity of effective 1D description. (a) Tetratomic binding energy as a function of Ω at a given $\xi = \pi/12$. E_2^B and E_2^F are exact solutions of bosonic and fermionic systems, and E_2^{1D} is from effective 1D model (9) with high-order angular fluctuations. Inset plot shows η , defined in (24), as a function of Ω . The horizontal line marks the location when η reduces to 5%, as also shown by the green arrow in the main plot. (b) Diagram for the validity of 1D description in (Ω, ξ) plane. Solid line shows the critical boundary when $\eta = 5\%$, and the 1D description is a good approximation in the green area above this boundary. The units of energy and Ω are respectively E_u and E_u/\hbar . The upper axis of Ω in (b) shows its absolute value [in unit of (2π) MHz] for NaK system.

define a dimensionless parameter

$$\eta = \left| \frac{E_2^B - E_2^F}{E_2^B + E_2^F} \right|,\tag{24}$$

which represents the relative deviation between E_2^B and E_2^F . As shown in the inset of Fig.2(a), η decreases rapidly with increasing Ω . We take the location where η reduces to 5% as the critical boundary for the validity of 1D description. In Fig.2(b), we map out this boundary in the parameter plane of (Ω, ξ) . The green area above this boundary is the validity regime of 1D model, where $\eta \leq 5\%$. Remarkably, we can see that the 1D model is valid across a wide range of Ω even at small ξ . Take NaK system as an example, the validity just requires

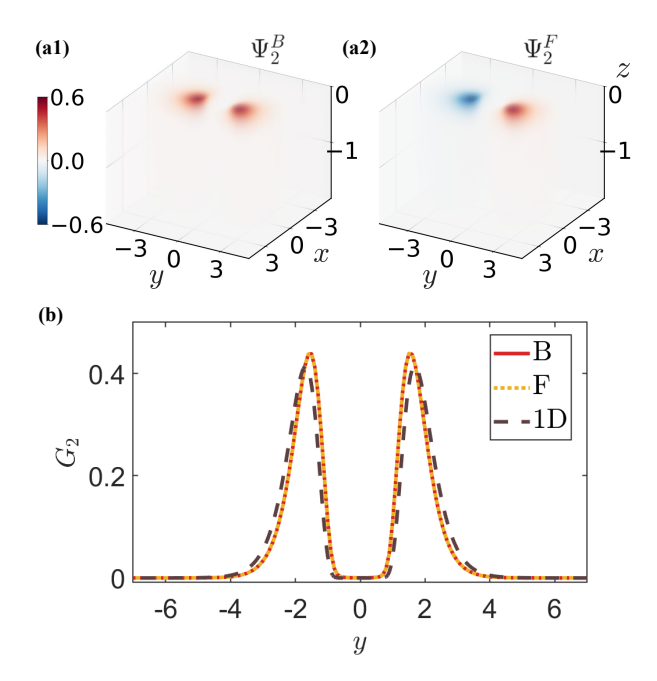


FIG. 3. Bose-Fermi duality of tetratomic bound states. (a1,a2) show the real-space wavefunctions of bosonic (Ψ_2^B) and fermionic (Ψ_2^F) systems from exact solutions, and (b) shows their reduced density correlation functions $G_2(y)$ (Eq.25), in comparison with results from the effective 1D model. Here we take $\xi = \pi/12, \hbar\Omega/E_u = 157$, and the length unit as l_u .

 $\Omega > (2\pi)5.4 \mathrm{MHz}$ for $\xi = \pi/12$, and $> (2\pi)38.3 \mathrm{MHz}$ for ξ as small as $\pi/30$. This shows that in practical situations with Ω of tens of MHz, the 1D model performs robustly well even for small microwave field ellipticities.

Similar to the highly elliptic case [48], the Bose-Fermi duality can be probed via the density-density correlation function along y:

$$G_2(y) \equiv \langle n(0)n(y)\rangle.$$
 (25)

As seen from its definition, $G_2(y)$ directly measures the probability of finding two molecules with relative distance y along the 1D direction. For the tetratomic system, we have $G_2(y) = \int dx dz |\Psi_2(\mathbf{r})|^2$ from exact 3D solutions and $= |F_0(y)|^2$ from effective 1D model. Taking a small $\xi = \pi/12$ and a typical $\hbar\Omega/E_u = 157$, in Fig.3(a,b) we plot the real-space wavefunctions of bosonic and fermionic systems, with their corresponding $G_2(y)$ shown in Fig.3(c). We can see that the exact G_2 for both bosonic and fermionic systems match very well with the 1D prediction, directly demonstrating Bose-Fermi duality in this case.

Despite duality in spectral and real space, bosonic and fermionic systems are typically distinguishable in momentum space. This is because the momentum-space wavefunction involves a transformation of real-space counterpart across different spatial ordering sectors, thereby successfully carrying the information of exchange statistics. As shown in Fig.4 (a1,a2), the two

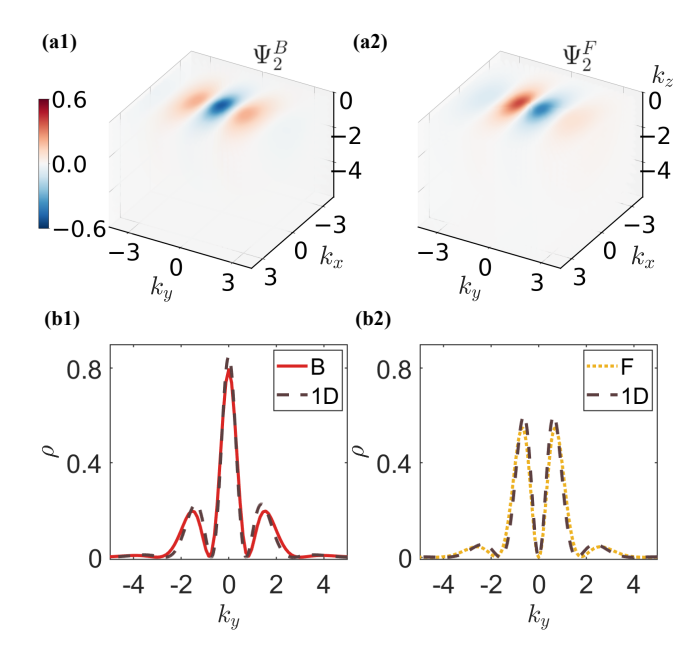


FIG. 4. Momentum-space distributions of tetratomic bound states. (a1,a2) show momentum-space wavefunctions for the lowest tetratomic bound states in bosonic (Ψ_2^B) and fermionic (Ψ_2^B) systems at $\xi = \pi/12$ and $\hbar\Omega/E_u = 157$. Accordingly, (b1,b2) show the reduced momentum-space distributions along k_y , from both exact solutions and effective 1D model. The length unit is l_u .

tetratomic systems indeed exhibit distinct momentumspace wavefunctions $\Psi_2^B(\mathbf{k})$ and $\Psi_2^F(\mathbf{k})$. Specifically, Ψ_2^B is most pronounced at $\mathbf{k}=0$ while Ψ_2^F is peaked at finite \mathbf{k} . As a result, the reduced momentum distributions along y, denoted by $\rho^{B/F}(k_y) = \int dk_x dk_z |\Psi_2^{B/F}(\mathbf{k})|^2$, are also very different, see Fig.4(b1,b2). Again, the exact $\rho^{B/F}$ agree very well with the predictions from effective 1D theory.

In cold atoms experiments, the real-space density correlation (25) can be probed via quantum gas microscopes[55–57], and the momentum distribution can be measured through time-of-flight imaging.

B. Born-Oppenheimer potential

In the previous section, we have examined the validity of effective 1D model for tetratomic bound state. This validity, however, does not automatically guarantee equal validity for hexatomic system. As we learn from fewbody physics in atomic gases, three-body systems can behave qualitatively differently from two-body ones. For example, three particles can support Efimov physics as facilitated by a scale-invariant $-1/R^2$ potential, which is absent in two-body sector. Therefore, it is necessary to independently examine the validity of 1D description for hexatomic system. In our previous study, we utilized the heavy-heavy-light molecular system to rule out Efimov physics and confirm the validity of effective 1D approach

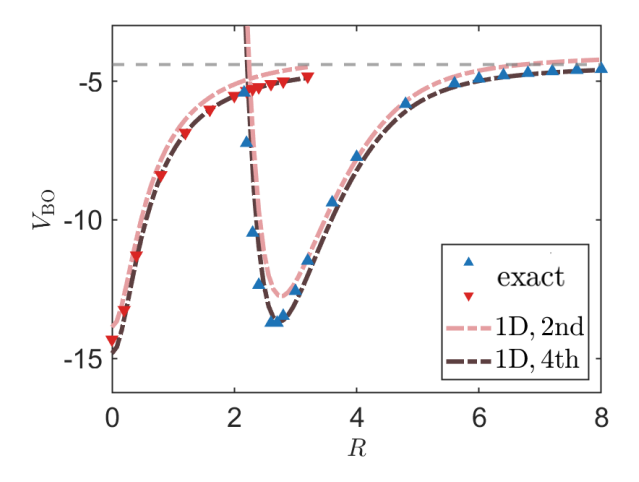


FIG. 5. Born-Oppenheimer potential $V_{\rm BO}({\bf R}=R\hat{y})$ between two heavy molecules mediated by the light one. Here we take $\xi=\pi/12$ and $\hbar\Omega/E_u=157$. Red and blue triangles show exact results of $V_{\rm BO}$ for two lowest eigen-levels. Pink and purple dashed lines are predictions from effective 1D models up to the second- and fourth-order angular fluctuations. The horizontal gray line shows the tetratomic binding energy of a heavy-light pair. The length and energy units are respectively l_u and E_u .

for a high microwave field ellipticity ($\xi = \pi/4$)[48]. Here we evaluate the validity of 1D approach to more realistic case of small ξ .

Taking a small $\xi = \pi/12$ and a typical $\hbar\Omega/E_u = 157$, we have exactly solved the Hamiltonian (11) to obtain the light-mediated heavy-heavy potential $V_{\rm BO}(\mathbf{R})$, with $\mathbf{R} = R\hat{y}$ pointing along the most attractive (y) direction. The two lowest levels of $V_{\rm BO}$ are shown in Fig.5 as functions of R, see red and blue triangles. As discussed in [48], these two orthogonal levels correspond to the light molecule residing besides (red) and in-between (blue) heavy ones, respectively. In Fig.5, these exact results are compared with predictions from effective 1D models up to the lowest- and high-order angular fluctuations. We can see that the inclusion of high-order fluctuations further improve the accuracy of 1D prediction compared to the lowest-order case, leading to excellent agreements with exact results across the entire regime of R.

We have also checked other parameters of ξ and Ω , and found the 1D model with high-order angular fluctuations accurately predict $V_{\rm BO}$ of heavy-heavy-light system for ξ and Ω lying within the green area of Fig.2(b). In this regime, the bound states are sufficiently deep and the system is far from scattering resonance with $a_s \to \infty$. This is why the Efimov physics is greatly suppressed while universal bound states, which depend only on the physical parameters l_d , ξ and Ω , are favored. The formation of these bound states is uniquely facilitated by the attractive potential along y, rather than by the large positive a_s near resonance.

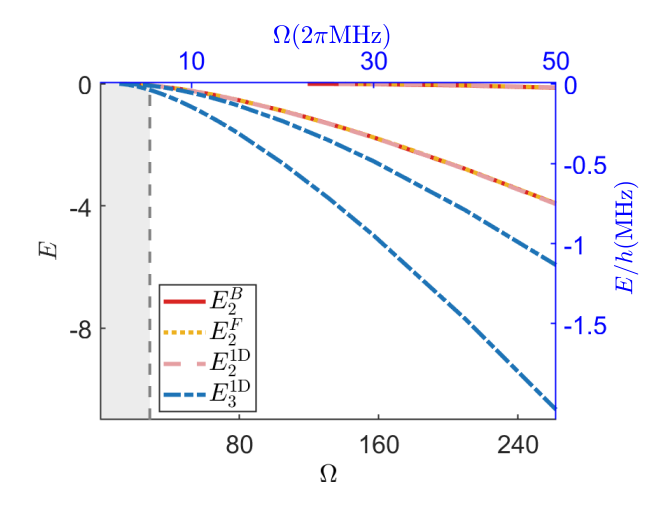


FIG. 6. Tetratomic and hexatomic bound state spectra at $\xi=\pi/12$. E_2^B and E_2^F are the exact tetratomic energies for bosonic and fermionic systems, in comparison with E_2^{1D} from effective 1D model (9). E_3^{1D} is the hexatomic energy from effective 1D model (23). For each of them, we have shown two lowest energy levels. The shaded area marks small Ω regime where the 1D description is invalid, i.e., lying in the white region of Fig.2(b). The units of Ω and E are respectively E_u/\hbar and E_u . Upper and right axes show the absolute values of Ω and E for NaK system.

C. Hexatomic bound state of three identical molecules

Given the accuracy of effective 1D model in reproducing tetratomic bound state and BO potential of heavy-heavy-light system, we can now confidently utilize it to study hexatomic bound state of three identical molecules. Here we take the parameters of ξ and Ω within the validity regime of 1D description (the green area in Fig.2(b)) and carry out exact diagonalization of effective 1D Hamiltonian (23) in discretized real space to obtain the hexatomic eigenstates. Given the hard-core nature of 1D potential in (23), the bosonic and fermionic systems obey Bose-Fermi duality, possessing identical energy spectra and real-space density profiles.

Fig.6 shows the bound state spectra of tetratomic and hexatomic systems as functions of Ω for a fixed $\xi=\pi/12$. Remarkably, we see that the hexatomic binding energies are generally much deeper than the tetratomic ones, for both ground and excited states. We emphasize that these hexatomic bound states are universal, not Efimovtype, as their binding energies do not depend on shortrange details but only on the physical parameters of dipole length (l_d) and microwave parameters (Ω, ξ) . Furthermore, they differ significantly from universal bound states in atomic systems, where a finite mass imbalance is required for trimer binding to dominate over dimer binding[6–14]. In contrast, the universal hexatomic bind-

ing revealed here requires no mass imbalance, a unique consequence of long-range interaction as we will discuss later.

The effective 1D description ensures the Bose-Fermi duality for hexatomic molecules. As shown in Fig.7(a1,a2), the wavefunctions of bosonic (Ψ_3^B) and fermionic (Ψ_3^F) systems differ only by symmetry in real space, while their density correlation functions, $G_2(y)$, are exactly identical, see Fig.7(c). The different exchange symmetries lead to distinct momentum-space wavefunctions, as shown in Fig.7(b1,b2) for bosonic and fermionic systems respectively. These distinctions can be probed via the single-particle momentum distribution along y, defined for a hexatomic system as

$$\rho^{B/F}(k) = \int dk_{\rho} |\Psi_3^{B/F}(k_r = -k - k_{\rho}/\sqrt{3}, k_{\rho})|^2.$$
 (26)

As shown in Fig.7(d1,d2), ρ^B and ρ^F both display visible crystalline patterns, but they are still well distinguishable: ρ^B is more pronounced at $k_y = 0$ while ρ^F is more equally distributed among different peaks.

Now we analyze why hexatomic binding is more favorable than tetratomic binding for microwave-shielded molecules. As previously discussed for $\xi = \pi/4[48]$, the hexatomic ground state can be well approximated by the product of two tetratomic states linked side-by-side. Specifically, for three molecules aligned along y in the order $y_1 < y_2 < y_3$, its ground state can be approximated as

$$\tilde{\Psi}_{3;g} = \Psi_{2;g}(y_{12})\Psi_{2;g}(y_{23}), \tag{27}$$

where $y_{ij} \equiv y_i - y_j$ is the relative distance, and $\Psi_{2;g}(y)$ is the ground state of tetratomic molecules with relative distance y. We find that the relation (27) remains valid for small ξ . Taking $\xi = \pi/12$ and a typical $\hbar\Omega/E_u = 157$, we compare the hexatomic wavefunction $\Psi_{3;g}$ with the simplified form $\tilde{\Psi}_{3;g}$ in Fig.7(a1,a2,b1,b2) and (A1,A2,B1,B2) for both bosonic and fermionic systems in real- and momentum space, finding reasonably good agreement. The agreement is also evident from the density correlation function and momentum distribution plotted in Fig.7(c) and (d1,d2).

Given the robust relation in (27), we can anticipate that the binding energy of the lowest hexatomic state is around twice the tetratomic energy, leading to a much deeper binding of hexatomic system as shown in Fig.6. Physically, the universal phenomenon of enhanced hexatomic binding relative to tetratomic one is a direct consequence of long-range interaction potential. Moreover, the rich crystalline patterns of hexatomic wavefunctions in both real- and momentum-space, shown in Fig.7, are also uniquely associated with long-range interactions. From a few-to-many perspective, these patterns of few-molecule systems may shed light on intriguing crystalline orders in large molecular ensembles.

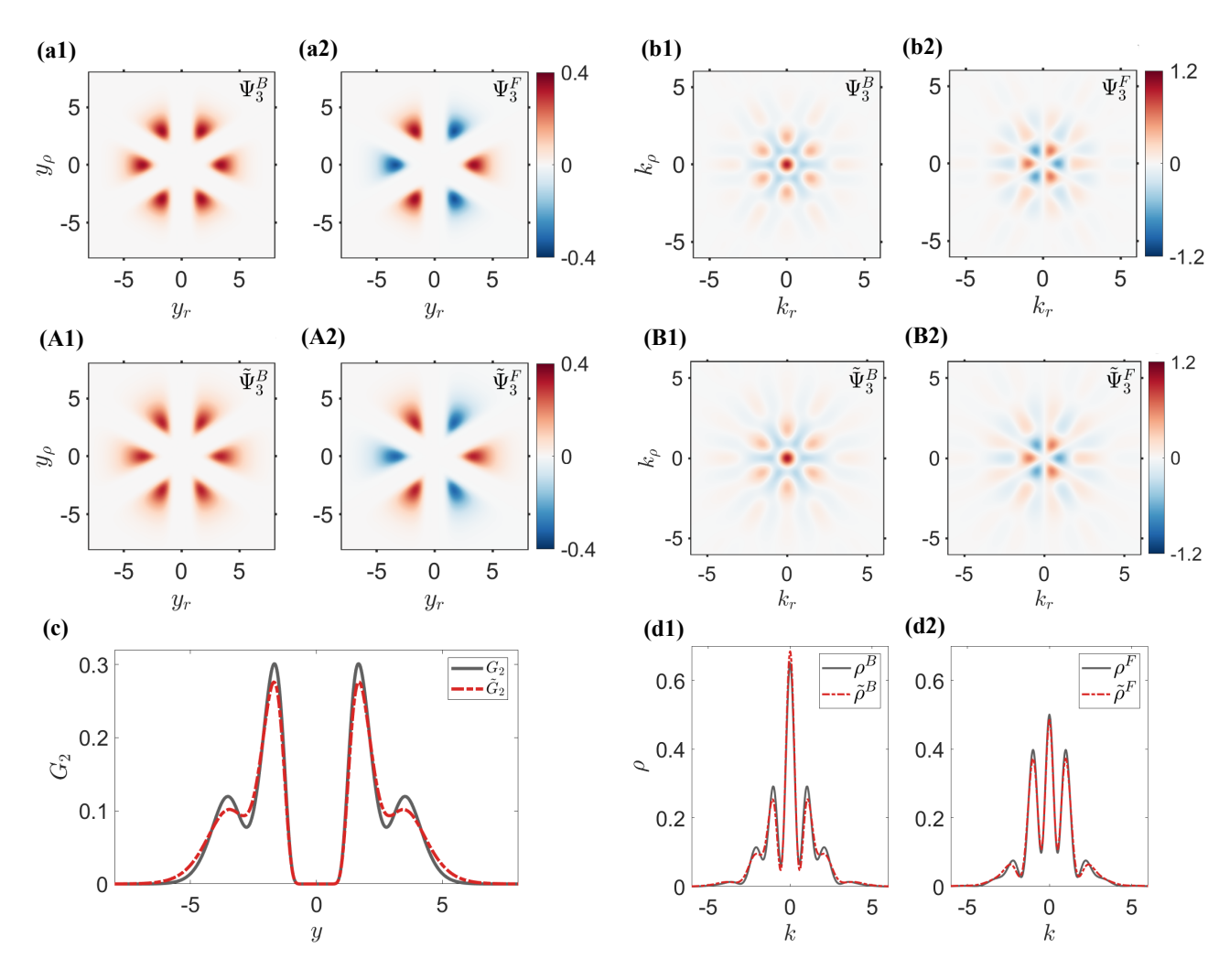


FIG. 7. Real- and momentum-space distributions of hexatomic ground state. Here we take $\xi = \pi/12$ and $\hbar\Omega/E_u = 157$. (a1,a2) and (b1,b2) show real- and momentum-space wavefunctions for bosonic (Ψ_3^B) and fermionic (Ψ_3^F) systems from the effective 1D model. In comparison, (A1,A2) and (B1,B2) show results from the simplified wavefunction in (27). (c) shows the density correlation function along y from the 1D model (G_2) and from the simplified wavefunction (\tilde{G}_2). (d1,d2) are the momentum distributions of bosonic (ρ^B) and fermionic (ρ^F) molecules from the 1D model, in comparison with results from the simplified wavefunction ($\tilde{\rho}^B$, $\tilde{\rho}^F$). The length unit is l_u .

The extension of (27) to large ensemble of molecules is straightforward: the ground state of N molecules is a product of N-1 nearest-neighbor tetratomic states linked along y direction, i.e., $\tilde{\Psi}_{N;g}$ $\Psi_{2;g}(y_{12})\Psi_{2;g}(y_{23})...\Psi_{2;g}(y_{N-1,N})$ for the spatial ordering $y_1 < y_2 ... < y_N$. The mean inter-molecule distance in $\Psi_{N;q}$ is roughly given by the minimum of effective 1D potential in Fig.1(c), which also determines the equilibrium density of this large bound state. In this sense, $\tilde{\Psi}_{N:a}$ constitutes a self-bound droplet with crystalline pattern along y direction. Visually, this state can be called as a "single-molecule array", which is universally applicable to both bosonic and fermionic systems. For fermionic system, this state is in sharp contrast to the conventional expectation of p-wave pairing superfluid as anticipated in previous experiment[25].

We have also computed the first excited hexatomic bound state, with spectrum shown in Fig.6. In Fig.8. we plot its typical real- and momentum-space wavefunctions for both bosonic and fermionic systems. Compared to the ground state in Fig.7, the excited state display very different crystalline patterns with more nodes in real and momentum space. In principle, this hexatomic excited state could be related to the tetratomic excited state, i.e., by replacing one tetratomic link from ground $(\Psi_{2;q})$ to excited state $(\Psi_{2;e})$. However, due to the very shallow $\Psi_{2;e}$ in this case (see Fig.6), the excited branch can no longer be considered as an isolated level for constructing the hexatomic excited state, which should instead involve a large amount of contributions from low-lying scattering states. Therefore, we do not explicitly construct the hexatomic excited state from isolated tetratomic levels

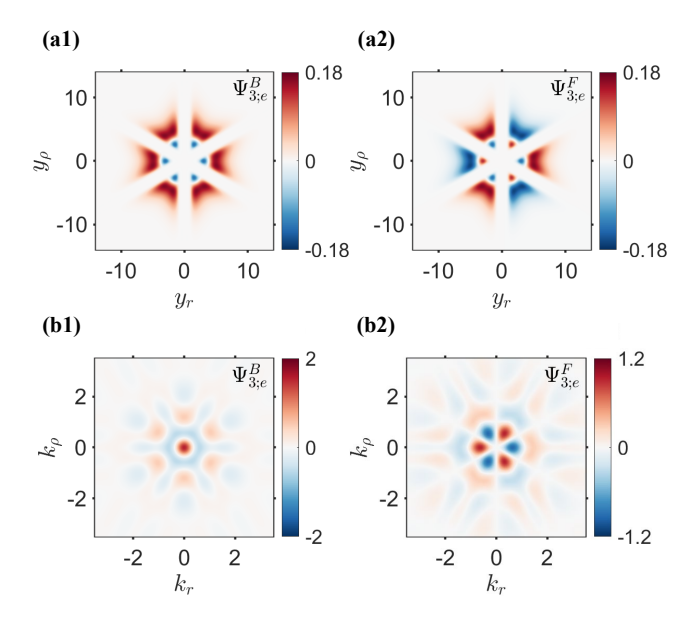


FIG. 8. Real- and momentum-space wavefunctions of the first excited hexatomic state. Here we take $\xi = \pi/12$ and $\hbar\Omega/E_u = 157$. (a1,a2) are the real-space wavefunctions of bosonic $(\Psi^B_{3;e})$ and fermionic $(\Psi^F_{3;e})$ systems, and (b1,b2) are their according momentum-space wavefunctions. The length unit is l_u .

here.

Finally, we discuss the possibility of observing Efimov trimers in bosonic molecules. As previously studied in dipolar systems[43], Efimov trimers can be supported near an s-wave resonance under the condition $|a_s| \gg l_d$. However, for current ultracold molecules with very large $l_d \sim 10^4 a_0$ [23–28], this condition is satisfied only within a narrow parameter region near resonance, as previously examined for $\xi = \pi/4$ [48]. In the present case with much smaller ξ , bound state formation is more difficult and thus Efimov trimers are expected to be even more fragile with parameter tuning. This makes the exploration of Efimov physics extremely challenging in current experiments of bosonic molecules. In comparison, the universal clusters revealed here are far more robust and practical to detect in realistic bosonic and fermionic molecular gases.

V. SUMMARY AND OUTLOOK

In summary, we have established a robust effective 1D theory for bound-state formation in 3D ultracold molecules under elliptic microwave shielding. Our results highlight the dimensional reduction purely through the anisotropy of long-range interaction potential, rather than through the application of any external confinement. A key finding is that high-order angular fluctuations have to be incorporated into the 1D model to achieve quantitative accuracy. This effective 1D description is remarkably robust across a wide range of coupling strengths at small ellipticities (Fig.2(b)). The

1D framework directly ensures a Bose-Fermi duality in tetratomic and hexatomic bound states, which can be directly probed via spectroscopy or correlation measurements. We also predict rich crystalline patterns in both real and momentum space, a unique feature supported by long-range interactions. Furthermore, by successfully constructing the hexatomic ground state from tetrameric units, we expect the ground state of a large system to be a self-bound droplet of many single molecules distributing along one direction with equal spacing. Such a "single-molecule array" is universally applicable to both bosonic and fermionic molecular systems.

A natural extension of this work is to investigate fewmolecule bound states in the limit of vanishing ellipticity $(\xi \to 0)$. In particular, a key question is the evolution of bound states as ξ is tuned to zero, a regime where the 1D description becomes inapplicable (see Fig.2(b)). For $\xi \to 0$, an effective 2D theory can be established by incorporating longitudinal fluctuations beyond the 2D plane, analogous to our present approach. Consequently, tuning ξ can drive a dimensional crossover from 1D to 2D, potentially giving rise to distinct crystalline patterns and a breakdown of Bose-Fermi duality. Moreover, another extension of the present work is to consider the dual microwave fields as implemented in bosonic molecules [28– 30]. Following the few-to-many roadmap, a solid fewbody study will offer a trustable path to explore complex many-body phases, a strategy particularly valuable for the field of ultracold molecules where few-body physics remains largely uncharted.

Methods

Tetratomic system:

The expansion of interaction potential $V(\mathbf{r})$ in (3) gives

$$\begin{split} V^{(0)}(r) &= -\left(1 + 3f_{\xi}\right)\frac{C_3}{r^3} + (1 - f_{\xi}^2)\frac{C_6}{r^6}; \\ V^{(2)}(r, \delta\theta, \delta\phi) &= \left(\frac{3C_3}{r^3} + \frac{2f_{\xi}C_6}{r^6}\right)\left((1 + f_{\xi})\delta\theta^2 + 2f_{\xi}\delta\phi^2\right); \\ V^{(4)}(r, \delta\theta, \delta\phi) &= -(1 + f_{\xi})\left(\frac{C_3}{r^3} + (1 + \frac{5f_{\xi}}{3})\frac{C_6}{r^6}\right)\delta\theta^4 \\ &- 2f_{\xi}\left(\frac{C_3}{r^3} + \frac{8f_{\xi}C_6}{3r^6}\right)\delta\phi^4 - 2f_{\xi}\left(\frac{3C_3}{r^3} + 2(2f_{\xi} + 1)\frac{C_6}{r^6}\right)\delta\theta^2\delta\phi^2. \end{split}$$

Similarly, the kinetic term $H_k = -\hbar^2 \nabla_{\mathbf{r}}^2 / m$ can be expanded as (4), with

$$\begin{split} H_k^{(0)}(r) &= -\frac{\hbar^2}{mr^2} \frac{\partial}{\partial r} \left(r^2 \frac{\partial}{\partial r} \right); \\ H_k^{(2)}(r, \delta\theta, \delta\phi) &= -\frac{\hbar^2}{mr^2} \left(\frac{\partial^2}{\partial \delta\theta^2} + \frac{\partial^2}{\partial \delta\phi^2} \right); \\ H_k^{(4)}(r, \delta\theta, \delta\phi) &= -\frac{\hbar^2}{mr^2} \left(-\delta\theta \frac{\partial}{\partial \delta\theta} + \delta\theta^2 \frac{\partial^2}{\partial \delta\phi^2} \right). \end{split}$$

Note that we have neglected terms like $\delta\theta^{2n-1}\frac{\partial}{\partial\delta\theta}$ and $\delta\theta^{2n}\frac{\partial^2}{\partial\delta\phi^2}$ with $n\geq 2$, which belong to higher-order corrections and contribute very little to the effective potential in small r regime.

In Eq.(6), the Hamiltonian $H_k^{(2)} + V^{(2)}$ describes two independent harmonic oscillators in terms of $\delta\theta$ and $\delta\phi$. The zero-point energy is given by $U_{\rm eff}^{(2)}$ in (7), and the corresponding wavefunction follows

$$\psi_0(y; \delta\theta, \delta\phi) = \left(\frac{\sqrt{mAr}}{\pi\hbar}\right)^{\frac{1}{2}} \left[2f_{\xi}(1+f_{\xi})\right]^{\frac{1}{8}}$$
$$\exp\left[-\frac{\sqrt{mAr}}{2\hbar}\left(\sqrt{1+f_{\xi}}\delta\theta^2 + \sqrt{2f_{\xi}}\delta\phi^2\right)\right]$$

where r=|y| and $A=\frac{3C_3}{r^3}+\frac{2f_{\xi}C_6}{r^6}$. Based on this, the fourth-order contribution of effective potential in (8) can be evaluated as

$$\begin{split} U_{\text{eff}}^{(4)}(r) &= \int d\delta\theta \int d\delta\phi \; \psi_0^*(H_k^{(4)} + V^{(4)})\psi_0 \\ &= -\frac{\hbar^2}{2mr^2} \left(1 - \sqrt{\frac{f_\xi}{2(1+f_\xi)}}\right) \\ &- \frac{\hbar^2}{2mAr^2} \left[\frac{3C_3}{r^3} + \frac{(3+13f_\xi)C_6}{2r^6}\right] \\ &- \frac{\hbar^2}{2mAr^2} \sqrt{\frac{f_\xi}{2(1+f_\xi)}} \left[\frac{3C_3}{r^3} + \frac{2(1+2f_\xi)C_6}{r^6}\right]. \end{split}$$

It shows that $U_{\rm eff}^{(4)}$ is always negative for all r, and in the limit $r \to 0$ it scales as $-1/r^2$, much smaller than $U_{\rm eff}^{(2)} \sim 1/r^4$ in (7).

Heavy-heavy-light system:

Explicitly, $H_L^{(0)}$ and $H_L^{(2)}$ in (12) follow

$$H_L^{(0)}(r) = -\frac{\hbar^2}{2mr^2} \frac{\partial}{\partial r} \left(r^2 \frac{\partial}{\partial r} \right)$$

$$+ \sum_{\sigma=\pm} \left[-\frac{(1+3f_{\xi})C_3}{r_{\sigma}^3} + \frac{(1-f_{\xi}^2)C_6}{r_{\sigma}^6} \right];$$

$$H_L^{(2)}(y, \delta\theta, \delta\phi) = -\frac{\hbar^2}{2mr^2} \left(\frac{\partial^2}{\partial \delta\theta^2} + \frac{\partial^2}{\partial \delta\phi^2} \right)$$

$$+ \sum_{\sigma=\pm} \frac{r^2 A_{\sigma}}{r_{\sigma}^2} \left[(1+f_{\xi})\delta\theta^2 + 2f_{\xi}\delta\phi^2 \right], \qquad (28)$$

where $A_{\sigma} = \frac{3C_3}{r_{\sigma}^3} + \frac{2f_{\xi}C_6}{r_{\sigma}^6}$. Note that in obtaining $H_L^{(2)}$, we have neglected the angular fluctuations of radial distance r_{\pm} and replaced it with $r_{\pm} = |y \pm R/2|$. In this way one

can recover the correct asymptotic behavior of effective potential when a heavy-light pair come close together $(r_{\pm} \to 0)$. We can see that $H_L^{(2)}$ is again composed by two separate harmonic oscillators in terms of $\delta\theta$ and $\delta\phi$. Its zero-point energy, which gives $U_{\rm L:eff}^{(2)}$, reads

$$U_{\rm L;eff}^{(2)}(r) = \left(\sqrt{1 + f_{\xi}} + \sqrt{2f_{\xi}}\right) \sqrt{\frac{\hbar^2}{2m} \sum_{\sigma=\pm} \frac{A_{\sigma}}{r_{\sigma}^2}}.$$

Besides, the corresponding fourth-order contribution of effective potential can be evaluated as

$$U_{\text{L:eff}}^{(4)}(y) = u_{\text{eff}}^{(4)}(r_{+}) + u_{\text{eff}}^{(4)}(r_{-})$$

with $u_{\text{eff}}^{(4)}(r) = U_{\text{eff}}^{(4)}(r)/2$. Three identical molecules: Explicitly, $H_3^{(0)}$ and $H_3^{(2)}$ in (18) follow

$$\begin{split} &H_{3}^{(0)}(r,\rho) = -\frac{\hbar^{2}}{mr^{2}}\frac{\partial}{\partial r}\left(r^{2}\frac{\partial}{\partial r}\right) - \frac{\hbar^{2}}{m\rho^{2}}\frac{\partial}{\partial \rho}\left(\rho^{2}\frac{\partial}{\partial \rho}\right) \\ &-\frac{(1+3f_{\xi})C_{3}}{r^{3}} + \frac{(1-f_{\xi}^{2})C_{6}}{r^{6}} \\ &+ \sum_{\sigma=\pm}\left(-\frac{(1+3f_{\xi})C_{3}}{r_{\sigma}^{3}} + \frac{(1-f_{\xi}^{2})C_{6}}{r^{6}}\right); \\ &H_{3}^{(2)}(y_{r},\delta\theta_{r},\delta\phi_{r};y_{\rho},\delta\theta_{\rho},\delta\phi_{\rho}) = -\frac{\hbar^{2}}{mr^{2}}\left(\frac{\partial^{2}}{\partial\delta\theta_{r}^{2}} + \frac{\partial^{2}}{\partial\delta\phi_{r}^{2}}\right) \\ &-\frac{\hbar^{2}}{m\rho^{2}}\left(\frac{\partial^{2}}{\partial\delta\theta_{\rho}^{2}} + \frac{\partial^{2}}{\partial\delta\phi_{\rho}^{2}}\right) + A\left[(1+f_{\xi})\delta\theta_{r}^{2} + 2f_{\xi}\delta\phi_{r}^{2}\right] \\ &+ \sum_{\sigma=\pm}\frac{A_{\sigma}r^{2}}{4r_{\sigma}^{2}}\left[(1+f_{\xi})\delta\theta_{r}^{2} + 2f_{\xi}\delta\phi_{r}^{2}\right] \\ &+ \sum_{\sigma=\pm}\frac{3A_{\sigma}\rho^{2}}{4r_{\sigma}^{2}}\left[(1+f_{\xi})\delta\theta_{\rho}^{2} + 2f_{\xi}\delta\phi_{\rho}^{2}\right] \\ &+ \sum_{\sigma=\pm}\frac{\sqrt{3}A_{\sigma}\sigma}{2r_{\sigma}^{2}}\left[(1+f_{\xi})r\rho\delta\theta_{r}\delta\theta_{\rho} + 2f_{\xi}y_{r}y_{\rho}\delta\phi\delta\phi_{\rho}\right]. \end{split}$$

Here we again neglect the angular fluctuations of radial distance r_{\pm} and directly replace it with $|\frac{y_r \pm \sqrt{3}y_{\rho}}{2}|$. We can see that $H_3^{(2)}$ is composed by two independent harmonic oscillators, while within each oscillator the two modes $(\{\delta\theta_r, \delta\theta_{\rho}\})$ or $\{\delta\phi_r, \delta\phi_{\rho}\}$ are entangled with each other. The corresponding zero-point energy $U_{3;\text{eff}}^{(2)}$ can be evaluated following the approach in Ref.[48].

References

V. N. Efimov, Weakly-bound states of three resonantly interacting particles, Yad. Fiz. 12, 1080 (1970).

^[2] V. N. Efimov, Energy levels of three resonantly interacting particles, Nucl. Phys. A210, 157 (1973).

^[3] E. Braatena, H.-W. Hammer, Universality in few-body

systems with large scattering length, Physics Reports, 428, 259 (2006).

^[4] C. H. Greene, P. Giannakeas, and J. Pérez-Ríos, Universal few-body physics and cluster formation, Rev. Mod.

- Phys. 89, 035006 (2017).
- [5] P. Naidon and S. Endo, *Efimov physics: a review*, Rep. Prog. Phys. **80**, 056001 (2017).
- [6] O. I. Kartavtsev and A. V. Malykh, Low-energy threebody dynamics in binary quantum gases, J. Phys. B 40, 1429 (2007).
- [7] D. Blume, Universal Four-Body States in Heavy-Light Mixtures with a Positive Scattering Length, Phys. Rev. Lett. 109, 230404 (2012).
- [8] B. Bazak and D. S. Petrov, Five-Body Efimov Effect and Universal Pentamer in Fermionic Mixtures, Phys. Rev. Lett. 118, 083002 (2017).
- [9] L. Pricoupenko and P. Pedri, Universal (1+2)-body bound states in planar atomic waveguides, Phys. Rev. A 82, 033625 (2010).
- [10] J. Levinsen and M. M. Parish, Bound States in a Quasi-Two-Dimensional Fermi Gas, Phys. Rev. Lett. 110, 055304 (2013).
- [11] R. Liu, C. Peng, and X. Cui, Universal tetramer and pentamer in two-dimensional fermionic mixtures, Phys. Rev. Lett. 129, 073401 (2022).
- [12] O. I. Kartavtsev, A. V. Malykh, and S. A. Sofianos, Bound states and scattering lengths of three twocomponent particles with zero-range interactions under one-dimensional confinement, J. Exp. Theor. Phys. 108, 365 (2009).
- [13] N. P. Mehta, Born-Oppenheimer study of two-component few-particle systems under one-dimensional confinement, Phys. Rev. A 89, 052706 (2014).
- [14] A. Tononi, J. Givois, and D. S. Petrov, Binding of heavy fermions by a single light atom in one dimension, Phys. Rev. A 106, L011302 (2022).
- [15] C. J. M. Mathy, M. M. Parish, and D. A. Huse, Trimers, molecules, and polarons in mass-imbalanced atomic Fermi gases, Phys. Rev. Lett. 106, 166404 (2011).
- [16] M. M. Parish and J. Levinsen, Highly polarized Fermi gases in two dimensions, Phys. Rev. A 87, 033616 (2013).
- [17] S. Endo, A. M. García-García and P. Naidon, Universal clusters as building blocks of stable quantum matter, Phys. Rev. A 93, 053611 (2016).
- [18] R. Liu, C. Peng, X. Cui, Emergence of Crystalline Fewbody Correlations in Mass-imbalanced Fermi Polarons, Cell Reports Physical Science 3, 100993 (2022).
- [19] R. Liu, W. Wang, X. Cui, Quartet Superfluid in Two-Dimensional Mass-Imbalanced Fermi Mixtures, Phys. Rev. Lett. 131, 193401 (2023).
- [20] T. Karman and J. M. Hutson, Microwave Shielding of Ultracold Polar Molecules, Phys. Rev. Lett. 121, 163401 (2018).
- [21] L. Lassabliere and G. Quemener, Controlling the Scattering Length of Ultracold Dipolar Molecules, Phys. Rev. Lett. 121, 163402 (2018).
- [22] L. Anderegg, S. Burchesky, Y. Bao, S. S. Yu, T. Karman, E. Chae, K.-K. Ni, W. Ketterle, and J. M. Doyle, Observation of Microwave Shielding of Ultracold Molecules, Science 373, 779 (2021).
- [23] A. Schindewolf, R. Bause, X.-Y. Chen, M. Duda, T. Karman, I. Bloch, and X.-Y. Luo, Evaporation of *Microwave-Shielded Polar Molecules to Quantum Degeneracy*, Nature (London) 607, 677 (2022).
- [24] X.-Y. Chen, A. Schindewolf, S. Eppelt, R. Bause, M. Duda, S. Biswas, T. Karman, T. A. Hilker, I. Bloch, and X.-Y. Luo, Field-linked resonances of polar molecules,

- Nature (London) 614, 59 (2023).
- [25] X.-Y. Chen, S. Biswas, S. Eppelt, A. Schindewolf, F. Deng, T. Shi, S. Yi, T. A. Hilker, I. Bloch, and X.-Y. Luo, *Ultracold field-linked tetratomic molecules*, Nature (London) 626, 283 (2024).
- [26] J. Lin, G. Chen, M. Jin, Z. Shi, F. Deng, W. Zhang, G. Quéméner, T. Shi, S. Yi, and D. Wang, *Microwave shielding of bosonic NaRb molecules*, Phys. Rev. X 13, 031032 (2023).
- [27] N. Bigagli, C. Warner, W. Yuan, S. Zhang, I. Stevenson, T. Karman, and S. Will, Collisionally stable gas of bosonic dipolar ground state molecules, Nat. Phys. 19, 1579 (2023).
- [28] N. Bigagli, W. Yuan, S. Zhang, B. Bulatovic, T. Karman, I. Stevenson, and S. Will, Observation of Bose-Einstein Condensation of Dipolar Molecules, Nature (London) 631, 289 (2024).
- [29] S, Zhang, W. Yuan, N. Bigagli, H. Kwak, T. Karman, I. Stevenson, S. Will, Observation of Self-Bound Droplets of Ultracold Dipolar Molecules, arxiv:2507.15208 (2025).
- [30] Z. Shi, Z. Huang, F. Deng, W.-J. Jin, S. Yi, T. Shi, D. Wang, Bose-Einstein condensate of ultracold sodiumrubidium molecules with tunable dipolar interactions, arxiv:2508.20518 (2025).
- [31] Z. Gu, X. Zhou, W. Chen, W. Han, F. Deng, T. Shi, P. Wang, and J. Zhang, Tetratomic states of microwave dressed and associated ultracold ²³Na⁴⁰K molecules, arXiv:2509.23634 (2025).
- [32] A. V. Avdeenkov and J. L. Bohn, Linking Ultracold Polar Molecules, Phys. Rev. Lett. 90, 043006 (2003).
- [33] A. V. Avdeenkov, D. C. E. Bortolotti, J. L. Bohn, Field-linked States of Ultracold Polar Molecules, Phys. Rev. A 69, 012710 (2004).
- [34] F. Deng, X.-Y. Chen, X.-Y. Luo, W. Zhang, S. Yi, and T. Shi, Effective Potential and Superfluidity of Microwave-Shielded Polar Molecules, Phys. Rev. Lett. 130, 183001 (2023).
- [35] G. Quéméner, J. L. Bohn, and J. F. Croft, Electroassociation of Ultracold Dipolar Molecules into Tetramer Field-Linked States, Phys. Rev. Lett. 131, 043402 (2023).
- [36] B.Mukherjee, M. D. Frye, C. R. Le-Sueur, M. R. Tarbutt, and J. M. Hutson, Shielding collisions of ultracold CaF molecules with static electric fields, Phys. Rev. Research 5, 033097 (2023).
- [37] B. Xu, F. Yang, R. Qi, H. Zhai, and P. Zhang, Synthetic Mutual Gauge Field in Microwave-Shielded Polar Molecular Gases Phys. Rev. Research 7, L032027 (2025).
- [38] J. Dutta, B. Mukherjee, J. M. Hutson, Universality in the microwave shielding of ultracold polar molecules, Phys. Rev. Research 7, 023164 (2025).
- [39] W. Jin, F. Deng, S. Yi, and T. Shi, Bose-einstein condensates of microwave-shielded polar molecules, Phys. Rev. Lett. 134, 233003 (2025).
- [40] W. Zhang, K. Chen, S. Yi, and T. Shi, Quantum phases for finite-temperature gases of bosonic polar molecules shielded by dual microwaves, PRX Quantum 6, 040307 (2025).
- [41] T. Langen, J. Boronat, J. Sanchez-Baena, R. Bombin, T. Karman, and F. Mazzanti, Dipolar droplets of strongly interacting molecules, Phys. Rev. Lett. 134, 053001 (2025).
- [42] M. Ciardi, K. R. Pedersen, T. Langen, and T. Pohl, Self-bound superfluid membranes and monolayer crystals of ultracold polar molecules Phys. Rev. Lett. 135, 153401

- (2025).
- [43] Y. Wang, J. P. D'Incao, and C. H. Greene, Efimov Effect for Three Interacting Bosonic Dipoles, Phys. Rev. Lett. 106, 233201 (2011).
- [44] Y. Wang, J. P. D'Incao, and C. H. Greene, Universal Three-Body Physics for Fermionic Dipoles, Phys. Rev. Lett. 107, 233201 (2011).
- [45] S.-J. Huang, Y.-T. Hsu, H. Lee, Y.-C. Chen, A. G. Volosniev, N. T. Zinner and D.-W. Wang, Field-induced longlived supermolecules, Phys. Rev. A 85, 055601 (2012).
- [46] K. Oi, P. Naidon, and S. Endo, Universality of Efimov states in highly mass-imbalanced cold-atom mixtures with van der Waals and dipole interactions, Phys. Rev. A 110, 033305 (2024).
- [47] I. Stevenson, S. Singh, A. Elkamshishy, N. Bigagli, W. Yuan, S. Zhang, C. H. Greene, and S. Will, Three-Body Recombination of Ultracold Microwave-Shielded Polar Molecules, Phys. Rev. Lett. 133, 263402 (2024).
- [48] T. Shi, H. Wang, and X. Cui, Universal Bound States with Bose-Fermi Duality in Microwave-Shielded Polar Molecules, arXiv:2504.21535 (2025).
- [49] T. Karman and J. M. Hutson, Microwave shielding of ultracold polar molecules with imperfectly circular polarization, Phys. Rev. A 100, 052704 (2019).
- [50] K. Kanjilal and D. Blume, Low-energy resonances and bound states of aligned bosonic and fermionic dipoles, Phys. Rev. A 78, 040703(R) (2008).
- [51] V. Roudnev and M. Cavagnero, Resonance phenomena in ultracold dipole-dipole scattering, J. Phys. B 42, 044017

- (2009).
- [52] Y. Wang, C. H. Green, Universal bound and scattering properties for two dipoles, Phys. Rev. A 85, 022704 (2012).
- [53] M.D. Girardeau, Relationship between systems of impenetrable bosons and fermions in one dimension, J. Math. Phys. 1, 516 (1960).
- [54] T. Cheon, T. Shigehara, Fermion-boson duality of onedimensional quantum particles with generalized contact interactions, Phys. Rev. Lett. 82, 2536 (1999).
- [55] T. de-Jongh, J. Verstraten, M. Dixmerias, C. Daix, B. Peaudecerf, and T. Yefsah, Quantum Gas Microscopy of Fermions in the Continuum, Phys. Rev. Lett. 134, 183403 (2025).
- [56] J. Xiang, E. Cruz-Colón, C. C. Chua, W. R. Milner, J. de-Hond, J. F. Fricke, and W. Ketterle, In situ imaging of the thermal de Broglie wavelength in an ultracold Bose gas, Phys. Rev. Lett. 134, 183401 (2025).
- [57] R. Yao, S. Chi, M. Wang, R. J. Fletcher, and M. Zwierlein, Measuring pair correlations in Bose and Fermi gases via atom-resolved microscopy, Phys. Rev. Lett. 134, 183402 (2025).

Acknowledgements

This work is supported by National Natural Science Foundation of China (12525412, 92476104, 12134015) and Quantum Science and Technology-National Science and Technology Major Project (2024ZD0300600).